

Chapter 4

POTENTIAL-WELL DISTORTION

4.1 THE GENERAL SOLUTION

In this chapter, we are going to study stationary bunch distributions, or distributions that are time independent. From the Vlasov equation depicted in Eq. (3.18), it is evident that the solution for the distribution $\psi(\tau, \delta E)$ must satisfy

$$[\psi, H] = 0 , \quad (4.1)$$

or ψ must be a function of the Hamiltonian,

$$\psi = \psi(H) . \quad (4.2)$$

Recall that the Hamiltonian of a particle with small amplitude synchrotron oscillations is

$$H = -\frac{\eta}{2v\beta^2 E_0}(\Delta E)^2 - \frac{\omega_{0s}^2 \beta^2 E_0}{2\eta v} \tau^2 + V(\tau) , \quad (4.3)$$

which describes the motion of the particle in the potential well

$$U(\tau) = -\frac{\omega_{0s}^2 \beta^2 E_0}{2\eta v} \tau^2 + V(\tau) . \quad (4.4)$$

When the effects of the wake potential is removed, this is just a parabolic potential well. In the presence of the wake potential, the potential well is distorted and the distribution of the beam particle in the longitudinal phase space is therefore modified. As will be

seen below, a purely reactive wake potential, meaning that the coupling impedance is either inductive or capacitive, will modify the parabolic potential in such a way that the potential well remains symmetric. Correspondingly, the distorted particle distribution will also be head-tail symmetric. A wake potential with a resistive component, however, will affect the symmetry of the parabolic potential well so that the bunch distribution will no longer be head-tail symmetric.

4.2 THE REACTIVE FORCE

Consider a beam with linear density $\rho(s-vt)$ traveling in the positive s direction inside a cylindrical beam pipe of radius b with infinitely conducting walls. We also assume at this moment that the beam is uniformly distributed transversely within a radius a which does not vary longitudinally. We are interested in the longitudinal electric field E_s seen by the beam particles at the axis of the beam. To compute that we invoke Faraday's law,

$$\vec{\nabla} \times \vec{E} = -\frac{\partial}{\partial t} \vec{B}, \quad (4.5)$$

or in the integral form,

$$\oint \vec{E} \cdot d\vec{\ell} = -\frac{\partial}{\partial t} \oint \vec{B} \cdot d\vec{A}. \quad (4.6)$$

In above, the closed path of integration of the electric field \vec{E} is along two radii of the beam pipe at s and $s + ds$ together with two length elements at the beam axis and the wall of the beam pipe, as illustrated in Fig. 4.1. The area of integration of the magnetic flux density \vec{B} is the area enclosed by the closed path. Now, the left side of Eq. (4.6) becomes

$$\text{L. S.} = E_s ds + \frac{e\rho(s+ds-vt)}{2\pi\epsilon_0} \left[\int_0^a \frac{rdr}{a^2} + \int_a^b \frac{dr}{r} \right] - \frac{e\rho(s-vt)}{2\pi\epsilon_0} \left[\int_0^a \frac{rdr}{a^2} + \int_a^b \frac{dr}{r} \right], \quad (4.7)$$

while the right side

$$\text{R. S.} = -\frac{\partial}{\partial t} \frac{\mu_0 e \rho(s-vt) v}{2\pi} \left[\int_0^a \frac{rdr}{a^2} + \int_a^b \frac{dr}{r} \right] ds. \quad (4.8)$$

Assumption has been made that the $1/\gamma$ open angle of the radial electric field is small compared with the distance ℓ over which the linear density changes appreciably, or $b/\gamma \ll \ell$. In terms of the the squared-bracketed expressions in Eqs. (4.7) and (4.8), we can define

$$g_0 = 2 \left[\int_0^a \frac{rdr}{a^2} + \int_a^b \frac{dr}{r} \right] = 1 + 2 \ln \frac{b}{a}, \quad (4.9)$$

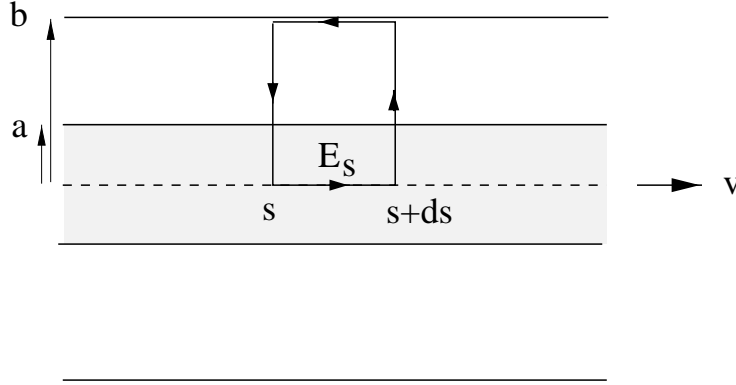


Figure 4.1: Derivation of the space-charge longitudinal electric field E_s experienced by a beam particle in a beam of radius a in an infinitely conducting beam pipe of radius b .

which is a geometric factor depending on the geometry of the beam and the beam pipe, and it will deviate from Eq. (4.9) if we relax, for example, the restriction of the transverse uniformity of the particle distribution. Combining the above, we arrive at

$$E_s + \frac{eg_0}{4\pi\epsilon_0} \frac{\partial\rho}{\partial s} = v^2 \frac{e\mu_0 g_0}{4\pi} \frac{\partial\rho}{\partial s}, \quad (4.10)$$

or

$$E_s = -\frac{eg_0}{4\pi\epsilon_0\gamma^2} \frac{\partial\rho}{\partial s}, \quad (4.11)$$

which is the space-charge force experienced by a particle in a beam.

The first application is a harmonic wave

$$\rho_1(s-vt) \propto e^{in(s/R-\omega_0 t)}, \quad (4.12)$$

perturbing a coasting beam of linear density ρ_0 , where n is the revolution harmonic and $v = R\omega_0$ with R being the radius of the accelerator ring. Substitution into Eq. (4.11) results in the voltage

$$V = -E_s C = \frac{ineZ_0cg_0}{2\gamma^2} \rho_1 \quad (4.13)$$

seen by a beam particle per accelerator turn. The perturbing wave constitutes a perturbing current $I_1 = e\rho_1 v$. Therefore, the space-charge impedance per harmonic seen is

$$\left. \frac{Z_0^\parallel}{n} \right|_{\text{sp ch}} = \frac{iZ_0g_0}{2\gamma^2\beta}, \quad (4.14)$$

which is to be compared with Eq. (1.30). From Eq. (4.11), the space-charge force experienced by a beam particle at position s and time t becomes

$$F(s, t) = \frac{ie^2 v}{2\pi} \frac{Z_0^\parallel}{n} \bigg|_{\text{sp ch}} \frac{\partial \rho(s, t)}{\partial s} . \quad (4.15)$$

Since an inductive impedance can be viewed as a negative space-charge impedance, we can write the force due to a general reactive impedance as

$$F(s, t) = \frac{ie^2 v}{2\pi} \frac{Z_0^\parallel}{n} \bigg|_{\text{reactive}} \frac{\partial \rho(s, t)}{\partial s} . \quad (4.16)$$

When the position of the beam particle is measured in terms of time advanced τ of some synchronous particles, the particle distribution $\lambda(\tau, t)$, which is normalized to the total number of beam particles, is related to $\rho(s, t)$ by

$$\rho(s, t) ds = \lambda(\tau, t) d\tau \quad \text{or} \quad \frac{\partial \rho(s, t)}{\partial s} = \frac{1}{v^2} \frac{\partial \lambda(\tau, t)}{\partial \tau} . \quad (4.17)$$

The reactive force exerted on a beam particle becomes

$$F(\tau, t) = \frac{ie^2}{2\pi v} \frac{Z_0^\parallel}{n} \bigg|_{\text{reactive}} \frac{\partial \lambda(\tau, t)}{\partial \tau} . \quad (4.18)$$

Of course, the above expression can also be obtained by substituting the reactive wake function

$$W'_0(\tau) = \delta'(\tau) \left[\frac{i}{\omega_0} \frac{Z_0^\parallel}{n} \right]_{\text{reactive}} \quad (4.19)$$

directly into Eq. (3.6).

The second application is on potential-well distortion. For a bunch, the head has a negative slope or $\partial \lambda / \partial \tau < 0$, while the tail has a positive slope or $\partial \lambda / \partial \tau > 0$. For a space-charge impedance, the head of the bunch is therefore accelerated and gains energy, while the tail decelerated and loses energy. Below transition, the head will arrive earlier after one turn while the tail arrives later, resulting in the spreading out of the bunch. The space-charge force therefore distorts the rf potential by counteracting the rf focusing force. On the other hand, an inductive force will help to enhance rf focusing. The opposite is true above transition.

4.3 HAISSINSKI EQUATION

For an electron bunch, because of the random quantum radiation and excitation, stationary distribution should have a Gaussian distribution in ΔE , or

$$\psi(\tau, \Delta E) = \frac{1}{\sqrt{2\pi}\sigma_E} \exp\left(-\frac{\Delta E^2}{2\sigma_E^2}\right) \rho(\tau) , \quad (4.20)$$

where σ_E is the rms beam energy spread determined by synchrotron radiation. Noting Eq. (4.2) and Hamiltonian in Eq. (4.3), we must have

$$\psi(\tau, \Delta E) \propto \exp\left(\frac{v\beta^2 E_0}{\eta\sigma_E^2} H\right) . \quad (4.21)$$

The linear density or distribution $\rho(\tau)$ is obtained by integrating over ΔE . Doing that, we finally arrive at a self-consistent equation for the line density, from, for example, Eqs. (3.16) and (3.17),

$$\rho(\tau) = \rho(0) \exp \left[- \left(\frac{\omega_{0s}\beta^2 E_0}{\eta\sigma_E} \right)^2 \frac{\tau^2}{2} + \frac{e^2\beta^2 E_0}{\eta T_0 \sigma_E^2} \int_0^\tau d\tau'' \int_{\tau''}^\infty d\tau' \rho(\tau') W'_0(\tau' - \tau'') \right] . \quad (4.22)$$

This is called the *Haissinski equation* [1], where the constant $\rho(0)$ is obtained by normalizing to the total number of particles in the bunch:

$$\int d\tau \rho(\tau) = N . \quad (4.23)$$

The solution will give a line distribution that deviates from the Gaussian form, and we call this the *potential-well distortion*. Since the rf voltage is modified, the synchrotron frequency also changes from $\omega_{0s}/(2\pi)$ to perturbed incoherent $\omega_s/(2\pi)$ accordingly.

For a purely resistive impedance $Z_0^\parallel(\omega) = R_s$, $W'_0(z) = R_s\delta(z/v)$, the equation can be solved analytically giving the solution [3]

$$\rho(\tau) = \frac{\sqrt{2/\pi} e^{-\tau^2/(2\sigma_\tau^2)}}{\alpha_R \sigma_\tau \{ \coth(\alpha_R N/2) - \text{erf}[\tau/(\sqrt{2}\sigma_\tau)] \}} , \quad (4.24)$$

where $\sigma_\tau = |\eta|\sigma_E/(\beta^2\omega_s E_0)$, $\alpha_R = e^2\beta^2 E_0 R_s/(\eta T_0 \sigma_E^2)$, and $\text{erf}(x) = (2/\sqrt{\pi}) \int_0^x e^{-t^2} dt$ is the error function. For a weak beam with $|\alpha_R|N \lesssim 1$, the peak beam density occurs at

$$\tau = \frac{\alpha_R N}{\sqrt{2\pi}} \sigma_\tau . \quad (4.25)$$

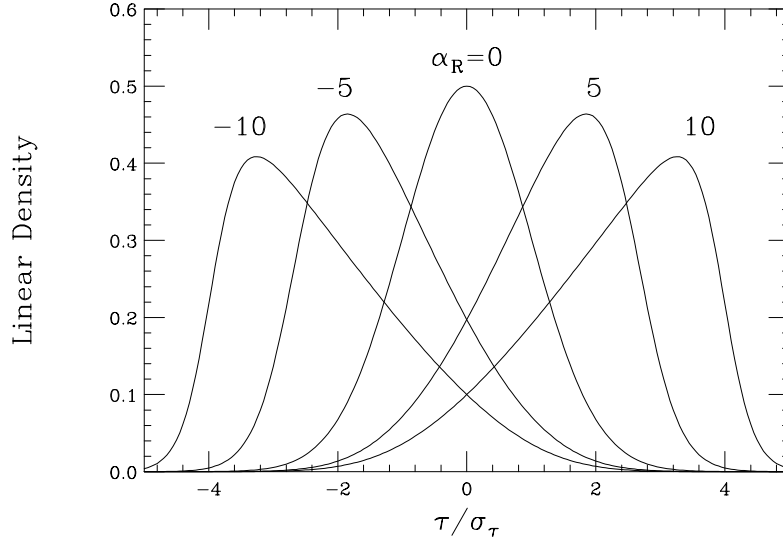


Figure 4.2: Plot of bunch profiles between $\pm 5 \sigma_s$ for $\alpha_R N = -10, -5, 0, 5$, and 10 , according to the solution of the Haissinski equation when the impedance is purely resistive. These profiles are normalized to $\sigma_\tau \sqrt{\pi/2}$ when integrated over τ . It is evident that the profile leans forward above transition ($\alpha_R > 0$) and backward below transition ($\alpha_R < 0$).

This peak moves forward above transition ($\alpha_R > 0$) and backward below transition ($\alpha_R < 0$) as the beam intensity increases. This effect comes from the parasitic loss of the beam particle which is largest at the peak of the linear density $\rho(\tau)$ and smallest at the two ends. Those particles losing energy will arrive earlier/later than the synchronous particle in time above/below transition and the distribution therefore lean forward/backward. Such bunch profiles are plotted in Fig. 4.2 for $\alpha_R N = -10, -5, 0, 5$, and 10 . In the plots, the linear densities are normalized to $\sigma_\tau \sqrt{\pi/2}$ when integrated over τ .

When the longitudinal impedance is purely inductive, $W'_0(z) = L\delta'(z/v)$, the Haissinski equation becomes

$$\rho(\tau) = k e^{-\tau^2/(2\sigma_\tau^2) - \alpha_L \rho(\tau)}, \quad (4.26)$$

where k is a positive constant and $\alpha_L = e^2 \beta^2 E_0 L / (\eta T_0 \sigma_E^2)$. Thus, $\rho e^{\alpha_L \rho}$ is an even function of τ , and it appears that the distorted distribution ρ is also an even function of τ . The line distribution will be left-right symmetric. Thus, the reactive part of the impedance will either lengthen or shorten the bunch, while the resistive part will cause the bunch to lean forward or backward. When $|\alpha_L|N \lesssim 1$, we can iterate,

$$\rho \approx k e^{-\tau^2/(2\sigma_\tau^2)} \left(1 - k \alpha_L e^{-\tau^2/(2\sigma_\tau^2)} \right). \quad (4.27)$$

In above, k represents the particle density at the center of the bunch. Now for $\alpha_L > 0$, effectively k becomes smaller. In other words, the distribution spreads out, or the effective rms bunch length becomes larger than σ_τ . This is the situation of either a repulsive inductive impedance force above transition or a repulsive capacitive force ($L < 0$) below transition. On the other hand, for an attractive inductive force below transition or an attractive capacitive force above transition, $\alpha_L < 0$ and the bunch will be shortened.

The longitudinal wake potential of the damping rings at the SLAC Linear Collider has been calculated carefully. Using it as input, the Haissinski equation is solved numerically at various beam intensities. The results are shown as solid curves in Fig. 4.3 along with the actual measurements. The agreement has been very satisfactory [2].

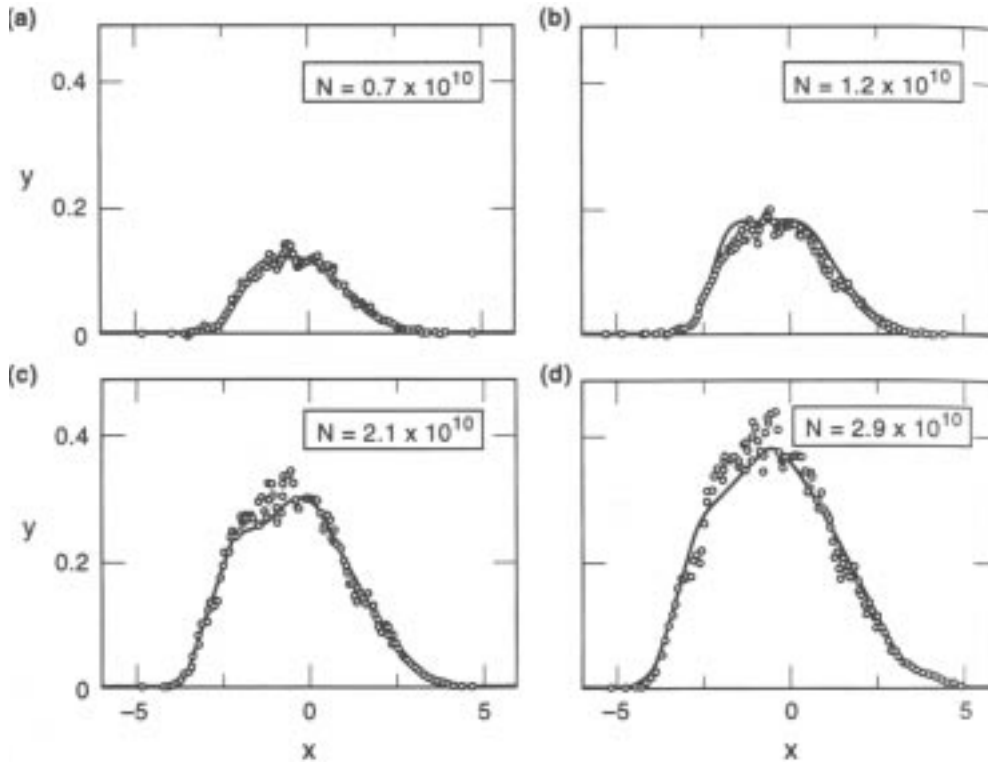


Figure 4.3: Potential-well distortion of bunch shape for various beam intensities for the SLAC SLC damping ring. Solid curves are solution of Haissinski solutions and open circles are measurements. The horizontal axis is in units of unperturbed rms bunch length σ_{z0} , while the vertical scale gives $y = 4\pi e\rho(z)/[V'_{rf}(0)\sigma_{z0}]$. The beam is going to the left.

4.4 ELLIPTICAL PHASE-SPACE DISTRIBUTION

An easier way to compute the bunch length distorted by the reactive impedance is to consider the elliptical phase-space distribution

$$\psi(\tau, \Delta E) = \frac{3N|\eta|\sqrt{\kappa}}{2\pi\beta^2\omega_s E_0 \hat{\tau}_0^3} \sqrt{\hat{\tau}_0^2 - \left(\frac{\eta}{\beta^2\omega_s E_0}\right)^2 \Delta E^2 - \kappa\tau^2} . \quad (4.28)$$

This distribution has a constant maximum energy spread of

$$\widehat{\Delta E} = \frac{\beta^2\omega_s E_0 \hat{\tau}_0}{|\eta|} , \quad (4.29)$$

which is determined by synchrotron radiation, while the half width of the bunch

$$\hat{\tau} = \frac{\hat{\tau}_0}{\sqrt{\kappa}} \quad (4.30)$$

is determined by the parameter κ . This distribution when integrated over ΔE gives the normalized parabolic line distribution

$$\rho(\tau) = \frac{3N\sqrt{\kappa}}{4\hat{\tau}_0^3} (\hat{\tau}_0^2 - \kappa\tau^2) . \quad (4.31)$$

With the reactive wake function $W'_0(z) = L\delta'(z/v)$, the Hamiltonian of Eq. (3.17) can therefore be written as a quadratic in ΔE and τ :

$$H = -\frac{\eta}{2v\beta^2 E_0} (\Delta E)^2 - \frac{\omega_s^2 \beta^2 E_0}{2\eta v} \tau^2 - \frac{e^2 L}{C} \rho(\tau) \quad (4.32)$$

$$= \frac{\omega_s^2 \beta^2 E_0}{2\eta v} \left[-\left(\frac{\eta}{\beta^2 \omega_s E_0}\right)^2 \Delta E^2 - \tau^2 (1 - D\kappa^{3/2}) \right] , \quad (4.33)$$

where

$$D = \frac{3e^2 N \eta v L}{2\omega_s^2 \beta^2 E_0 C \hat{\tau}_0^3} . \quad (4.34)$$

To be self-consistent, the expression of ψ in Eq. (4.28) must be a function of the Hamiltonian. Comparing Eq. (4.28) with Eq. (4.33), we arrive at

$$\kappa = 1 - D\kappa^{3/2} \quad (4.35)$$

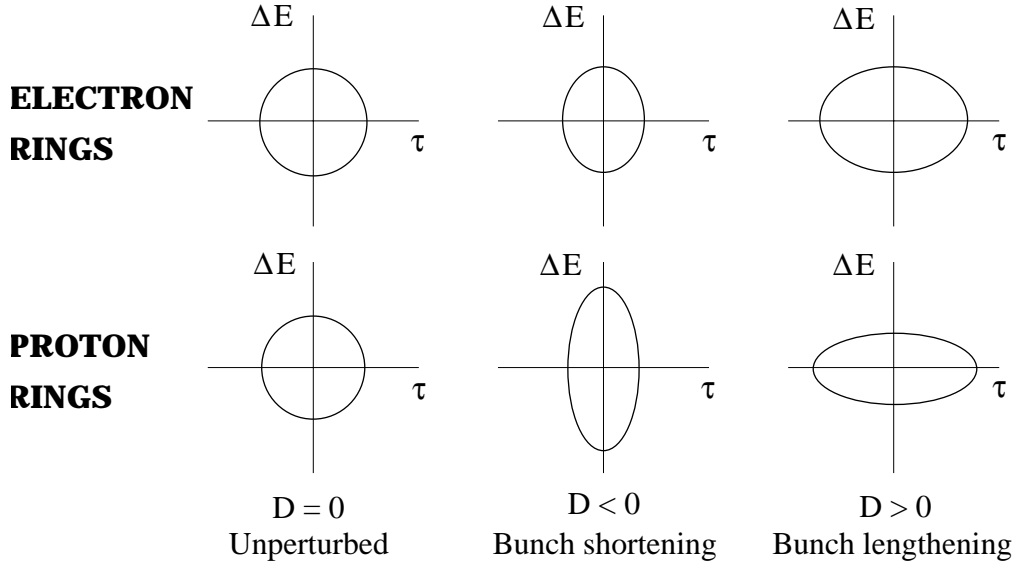


Figure 4.4: Potential well distortion of the bunch shape in the longitudinal phase space. $D > 0$ corresponds to either an inductive perturbation above transition or a capacitive perturbation below transition, while $D < 0$ implies either an inductive perturbation below transition or a capacitive perturbation above transition. Top row is for electron rings where the energy spread remains constant as a result of radiation damping. Bottom row is for proton rings where the bunch area is constant.

or

$$\left(\frac{\hat{\tau}}{\hat{\tau}_0}\right)^3 = \left(\frac{\hat{\tau}}{\hat{\tau}_0}\right) + D. \quad (4.36)$$

This cubic can be solved by iteration. First we put $\hat{\tau}/\hat{\tau}_0 = 1$ on the right side. If $D > 0$, we find $\hat{\tau}/\hat{\tau}_0 > 1$ or the bunch is lengthened. If $D < 0$, it is shortened. The former corresponds to either an inductive force above transition or a capacitive force below transition. The latter corresponds to either an inductive force below transition or a capacitive force above transition. This is illustrated in the first row of Fig. 4.4, where we notice that the energy spread of the bunch is unchanged for various types of perturbation.

For a proton bunch, the energy spread is also modified but the bunch area remains constant. The phase-space distribution has to be rewritten as

$$\psi(\tau, \Delta E) = \frac{3N|\eta|}{2\pi\beta^2\omega_s E_0 \hat{\tau}_0^3} \sqrt{\hat{\tau}_0^2 - \frac{1}{\kappa} \left(\frac{\eta}{\beta^2\omega_s E_0}\right)^2 \Delta E^2 - \kappa\tau^2}. \quad (4.37)$$

Now we have

$$\hat{\tau} = \frac{\hat{\tau}_0}{\sqrt{\kappa}} \quad \text{and} \quad \widehat{\Delta E} = \sqrt{\kappa} \widehat{\Delta E}_0 . \quad (4.38)$$

Again comparing with the Hamiltonian, we arrive at the quartic equation

$$\left(\frac{\hat{\tau}}{\hat{\tau}_0} \right)^4 = 1 + D \left(\frac{\hat{\tau}}{\hat{\tau}_0} \right) . \quad (4.39)$$

This is illustrated in the bottom row of Fig. 4.4.

4.5 COMPENSATING OF POTENTIAL-WELL DISTORTION

Potential-well distortion can often be a serious problem in the operation of an accelerator or storage ring. If the distortion opposes the rf bunching, a much larger rf voltage and hence rf power will be required to counteract the distortion. Even when compensated by a higher rf voltage, the rf bucket may have been so much distorted that its useful area has very much been reduced. An example is the Los Alamos PSR, which stores an intense proton beam at the kinetic energy of 797 MeV. The ring has a transition gamma of $\gamma_t = 3.1$, implying that the operation of the ring is below transition. The longitudinal space-charge force is therefore repulsive in nature and tends to lengthen the bunch. This longitudinal repulsive force will counteract the rf bunching force. We will study how serious the potential-well distortion is and possible way to cure the problem.

The PSR has a circumference of 90.2 m. It receives chopped proton beams from a linac in 1000 to 2000 turns. The beam is bunched by a rf buncher to the desired length and is then extracted for experimental use. The rf buncher is of rf harmonic $h = 1$, or there is only one bunch. The revolution frequency and the rf frequency are both 2.796 MHz. A typical store consists of a bunch consisting of 3.2×10^{13} protons, of half length $\hat{\tau} = 133.5$ ns, occupying roughly two third of ring, and a half energy spread of $\widehat{\Delta E}/E_0 = 0.005$. If space charge is neglected, to keep such a bunch matched to the rf bucket, the synchrotron tune is

$$\nu_{0s} = \frac{|\eta| \widehat{\Delta E}_0}{\omega_0 \beta^2 E \hat{\tau}} = 0.000402 , \quad (4.40)$$

and the required rf voltage is

$$V_{\text{rf}} = \frac{2\pi\beta^2 E_0 \nu_{0s}^2}{|\eta|h} = 6.60 \text{ kV} . \quad (4.41)$$

Now let us estimate the space-charge effect [4]. The 95% (or full) normalized transverse emittance is $50 \times 10^{-6} \pi \text{m}$. From this and the ring lattice, the g_0 factor has been estimated to be

$$g_0 = 1 + 2 \ln \frac{b}{a} \approx 3.0 , \quad (4.42)$$

where a is the beam radius and b the beam pipe radius. The longitudinal space-charge impedance is therefore

$$\left(\frac{Z_0^\parallel}{n} \right)_{\text{spch}} = i \frac{Z_0 g_0}{2\gamma^2 \beta} \approx i 196 \Omega . \quad (4.43)$$

according to Eq. (4.18), a particle with an arrival time τ ahead of the synchronous particle sees an electric field

$$E_{s \text{ spch}} = - \frac{e}{2\pi\beta c} \left| \frac{Z_0^\parallel}{n} \right|_{\text{spch}} \frac{d\lambda}{d\tau} , \quad (4.44)$$

where $\lambda(\tau)$ is the linear particle density of the bunch and is normalized to the number of particle in the bunch by integrating over τ . This electric field comes from the longitudinal space-charge effect and is in the direction of the motion of the bunch. It is positive in the head half of the bunch ($\tau > 0$) and negative in the tail half ($\tau < 0$). It is therefore repulsive. Assume a parabolic distribution,

$$\lambda(\tau) = \frac{3N}{4\hat{\tau}} \left(1 - \frac{\tau^2}{\hat{\tau}^2} \right) , \quad (4.45)$$

so that the electric field becomes linear in τ . The particle will gain in a turn the potential

$$V_{\text{spch}} = E_{s \text{ spch}} C = \frac{3eN}{2\omega_0 \hat{\tau}^2} \left| \frac{Z_0^\parallel}{n} \right|_{\text{spch}} \frac{\tau}{\hat{\tau}} = 4.82 \frac{\tau}{\hat{\tau}} \text{ kV} , \quad (4.46)$$

according to its position in the bunch. This potential is of roughly the same size as the rf voltage required if there is no space charge. Thus, in the presence of space charge, we need to increase V_{rf} from 6.60 kV to approximately $6.60 + 4.82 = 11.42$ kV; nearly 42% of the rf voltage has been spent to counteract the space-charge force. One must realize that the rf buncher at PSR was capable to deliver only 12 kV in 1997. Although the rf buncher has been upgraded to about 18 kV, there is also a goal to increase the beam intensity to 5×10^{13} protons as well.

4.5.1 FERRITE INSERTION

It has been proposed that if ferrite rings (also called cores) are installed inside the

vacuum chamber, the proton beam will see an extra inductive impedance from the ferrite, and hopefully this inductive impedance will cancel the capacitive space-charge impedance of the beam [5, 6]. Toshiba M_4C_{21A} ferrite rings are used, each having an inside diameter $d_i = 12.7$ cm, outside diameter $d_o = 20.3$ cm, and thickness $t = 2.54$ cm. The relative magnetic permeability is $\mu' \approx 70$ at the PSR rotation frequency, 2.796 MHz. For n_f ferrite rings stacked together, the impedance per harmonic is

$$\frac{Z_0^{\parallel}}{n_{\text{ferrite}}} = -i \frac{Z_0 \omega_0 t n_f}{2\pi c} \mu' \ln \frac{d_o}{d_i} = 2.93 n_f \Omega . \quad (4.47)$$

Thus, to cancel a space-charge impedance per harmonic of $\sim 300 \Omega$, about $n_f = 102$ will be needed. Three ferrite inserts were assembled. Each consisted of a stainless-steel pill-box cavity having an inner diameter of 20.3 cm and inner length of 75.5 cm, so that 30 ferrite cores could be packed inside. To prevent charge buildup on the inner surface of the cores, each of the cores were treated with a very thin (1 M Ω per square) conductive coating (Heraeus R8261) baked on the inner and outer surface. Additional radial conducting ‘spokes’ were added to provide conductivity from the inner surface to the outer wall of the chamber. Solenoidal wiring was wound outside the stainless steel container so that the magnetic permeability of the ferrite could be controlled.

Two such ferrite tuners or inserts were installed in the PSR in 1997. To study space-charge compensation caused by the installed inductance, two experiments, using different bunch lengths, were completed. The designated charge configurations were injected into the PSR and the longitudinal profiles (bunch length and shape) were observed, digitized, and recorded using signals from a wide-band wall current monitor at the end of each 625- μ s injection period. The experiments were performed for two bunch lengths: ~ 50 ns (half length) with 4.0×10^{12} particles and ~ 150 ns (half length) with 1.2×10^{13} . The rf voltage was set to 7 kV in both cases. The resulting waveforms are compared with detailed particle tracking simulations in Fig. 4.5 for the two bunch lengths. The solid curve in the top left plot represents the bunch shape with the full effect of the inserted inductance (zero bias). The dotted curve corresponds to data with the effect of the inductance diminished by 900-A dc bias. The difference of peak heights is about 16%. Simulations performed with assumed injection momentum spread $\Delta p/p = 0.08\%$ are shown in the top right plot. They predict an rms bunch length of 19 ns, but increasing to 22 ns when the ferrite bias current is raised to 900 A with the inductance reduced to 34% of its unbiased value. We see that the experiment measurements are consistent with the simulation predictions. Similar conclusion can be drawn for the long-bunch-length situation shown in bottom plots of Fig. 4.5. We see that bunch lengths have been reduced with the ferrite insertion,

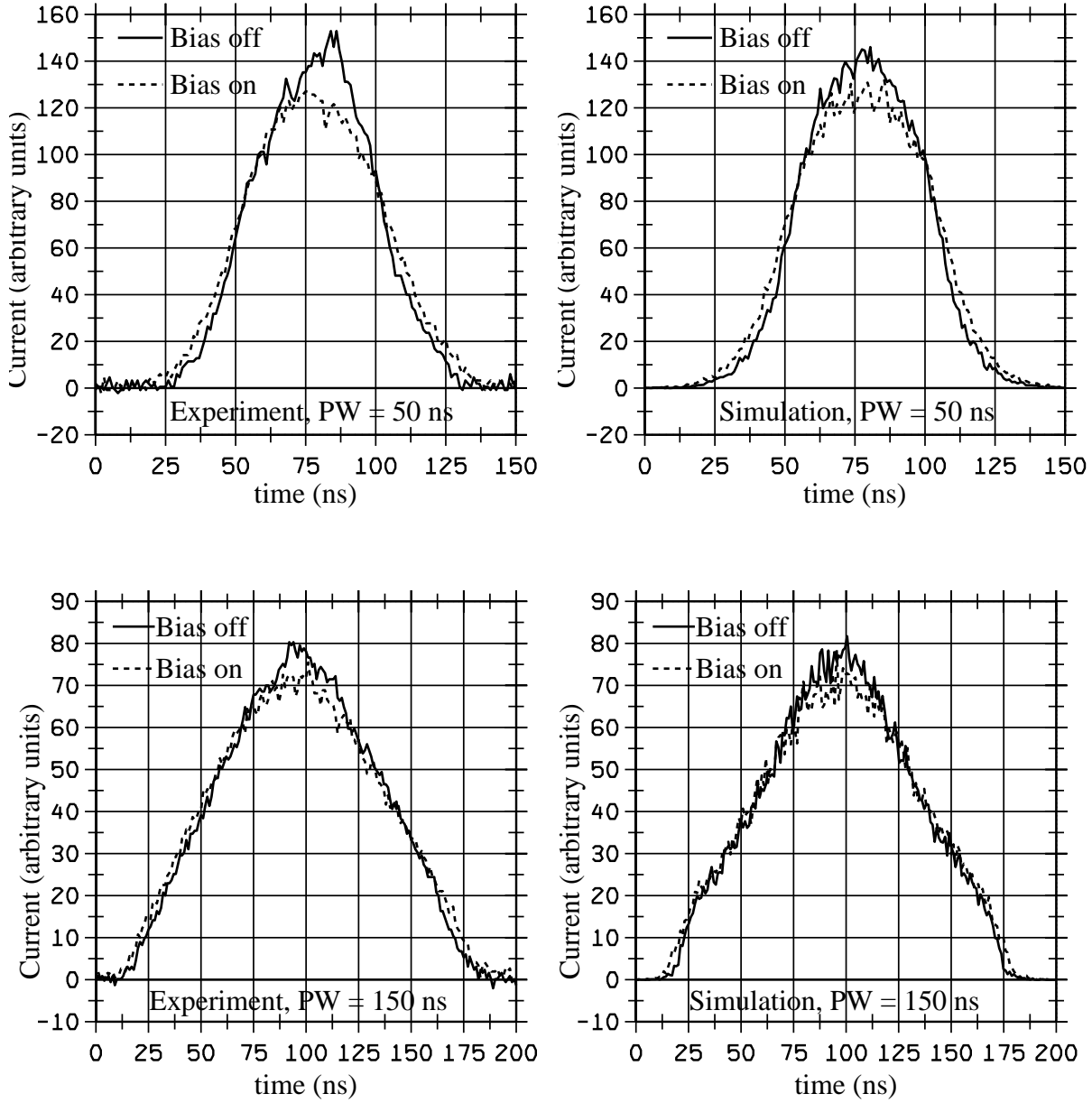


Figure 4.5: Measured (left) and simulated (right) pulse shapes after $625 \mu\text{s}$, for injected pattern widths of 50 ns with 4.0×10^{12} protons (bottom) and 150 ns with 1.2×10^{13} protons. In both cases, $V_{\text{rf}} = 7.5 \text{ kV}$. Solid: no bias, dotted: 900-A bias or a reduction of μ' by factor of 34%.

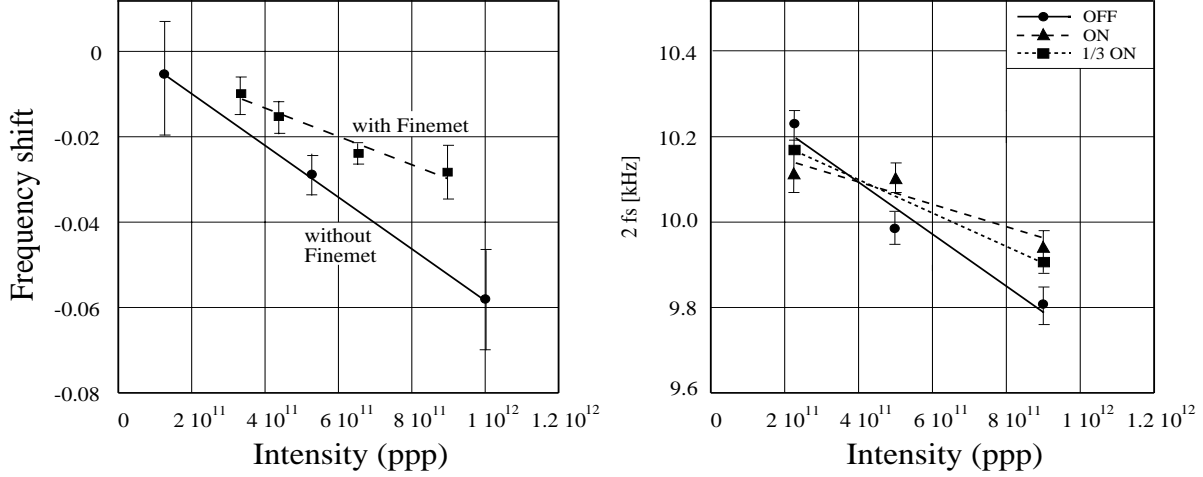


Figure 4.6: Left: Measured frequency shifts of the quadrupole oscillations versus beam intensity at KEK with and without Finemet. Right: New KEK results of quadrupole oscillation frequency versus beam intensity with Finemet tuners on, $\frac{1}{3}$ on, and off.

indicating that the space-charge impedance has been cancelled to a certain extent.

It is unfortunate that we cannot measure the change in synchrotron frequency so as to demonstrate the cancellation of space charge. This is mainly due to the slow synchrotron oscillation in the PSR. During the whole storage time, the beam particles usually make less than one synchrotron oscillation. A similar experiment has also been performed at the KEK PS Main Ring, but with a much lower intensity of 2 to 9×10^{11} protons per bunch [7]. The beam kinetic energy was 500 MeV with a space-charge impedance $Z_0^{\parallel}/n = i310 \Omega$. Instead of ferrite, a Met-Glass-like material called Finemet was used. The coherent frequency of the quadrupole synchrotron oscillation was measured as a function of bunch intensity. As shown in Fig. 4.6, with the inductor tuner on, the coherent frequency was less dependent on intensity, indicating that the space-charge force had been partially cancelled.

The second experiment at PSR is to measure the onset of vertical instability using a short-stripline beam-position monitor. With a 3.0×10^{13} proton beam stored, the rf voltage was lowered until vertical instability was registered. This signal comes about when the rf bucket is not large enough to hold the bunch so that some protons spill out into the bunch gap. These protons trap electrons preventing them to be cleared and causing a transverse e-p instability. It was found that, at the highest beam intensity the required rf

voltage was reduced to 60% of what had previously been necessary to maintain stability. This result indicates that the space-charge impedance has been compensated to a certain extent by the ferrite cores installed in the vacuum chamber. Thus, less rf voltage will be required to bunch the proton beam. The compensation of the potential-well distortion, however, was far from being perfect. This is because a longitudinal instability has been observed. At the intensity of 3.2×10^{13} protons, this instability has been small and appears to be tolerable. When the beam intensity was upgraded, however, the instability had been so intense that the beam profiles became heavily distorted and there was a considerable of beam loss. This instability together with its eventual cure will be discussed in detail in Sec. 5.7.

4.6 EXERCISES

4.1. Transform the Haissinski equation (4.22) according to the following:

(1) Notice that the integral over τ'' can be rewritten as

$$\int_0^\tau d\tau'' \rightarrow - \int_\tau^\infty d\tau'' , \quad (4.48)$$

where the extra constant can be absorbed into the normalization constant $\rho(0)$ which we rename by ξ .

(2) The integration in the τ' - τ'' space is in the 0° to 45° quadrant between the lines $\tau'' = \tau$ and $\tau'' = \tau'$. Translate the τ' and τ'' axes so that the region of integration is now between the τ' -axis and the 45° line $\tau'' = \tau'$.

(3) Integrate over τ'' first from 0 to τ' ; then integrate over τ' .

(4) Change the variable τ'' to $\tau' - \tau''$. Now the Haissinski equation takes the more convenient form

$$\rho(\tau) = \xi \exp \left[- \left(\frac{\omega_s \beta^2 E_0}{\eta \sigma_E} \right)^2 \frac{\tau^2}{2} - \frac{e^2 \beta^2 E_0}{\eta T_0 \sigma_E^2} \int_0^\infty d\tau' \rho(\tau + \tau') \int_0^{\tau'} d\tau'' W'_0(\tau'') \right] . \quad (4.49)$$

Notice that $\rho(\tau)$ on the left side only depends on the ρ on the right side evaluated in front of τ . We can therefore solve for ρ at successive slices of the bunch by assigning zero or some arbitrary value to ρ at the very first slice (the head) and some value to the constant ξ . The value of ξ is varied until the proper normalization of ρ is obtained.

4.2. The bunch in the Fermilab Tevatron contains $N = 2.7 \times 10^{11}$ protons and has a designed half length of $\hat{\tau} = 2.75$ ns. The ring main radius is $R = 1$ km and the slip

factor is $\eta = 0.0028$ at the incident energy of $E_0 = 150$ GeV. The rf harmonic is $h = 1113$ and the rf voltage is $V_{\text{rf}} = 1.0$ MV. Assume a broad-band impedance centered at $\omega_r/(2\pi) \approx 3$ GHz, quality factor $Q = 1$, and shunt impedance $R_s = 250$ k Ω .

(1) Show that the frequencies that the bunch samples are much less than the resonant frequency of the broad-band, so that the asymmetric beam distortion driven by $\text{Re } Z_0^{\parallel}$ can be neglected. (2) Using only the inductive part of the impedance at low frequencies, compute from Eq. (4.39) the equilibrium bunch length as a result of potential-well distortion. (3) Electron bunches are usually very short. If an electron bunch of rms bunch length 2 cm is put into the Tevatron, show that its spectrum will sample the resonant peak of $\text{Re } Z_0^{\parallel}$ and thus suffer asymmetric distortion. Verify this by substituting the data into Eq. (4.24).

- 4.3. From Eq. (4.36) for an electron bunch, show that there are two solutions for the perturbed bunch length due to distortion by a capacitive impedance when $-2/3^{3/2} < D < 0$. Which one is physical? When $D < -2/3^{3/2}$, there is no solution. At this critical situation, the bunch shortening ratio is $3^{-1/2}$.

Hint: Transform Eq. (4.36) to

$$4x^3 - 3x = \frac{3^{3/2}}{2}D \quad (4.50)$$

and substitute for $x = \sin \theta$. What is the right side in terms of θ ?

- 4.4. When the coupling impedance is purely resistive,
 (1) derive the potential-well distorted linear distribution, Eq. (4.24).
 (2) Show that when the intensity of the bunch is weak, the peak of the distribution is given by Eq. (4.25).

Hint: Transform the Haissinski equation to a differential equation,

$$\rho' + \frac{\tau}{\sigma_\tau^2} \rho - \alpha_R \rho^2 = 0 . \quad (4.51)$$

Solve the equation and determine $\rho(0)$.

Bibliography

- [1] J. Haissinski, *Nuovo Cimento* **18B**, 72 (1973).
- [2] K.L.F. Bane and R.D. Ruth, *Proc. IEEE Conf. Part. Accel.*, Chicago, 1989, p.789.
- [3] A.G. Ruggiero, *IEEE Trans. Nucl. Sci.* **NS-24**, 1205 (1977).
- [4] K.Y. Ng and Z. Qian, *Instabilities and Space-Charge Effects of the High-Intensity Proton Driver*, Fermilab Report FN-659, 1997, AIP Conference Proceedings 435, Workshop on Physics at the First Muon Collider and at the Front End of the Muon Collider, Ed. S. Geer and R. Raja, Batavia, IL, Nov. 6-9, 1997, p. 841.
- [5] J.E. Griffin, K.Y. Ng, Z.B. Qian, and D. Wildman, Fermilab Report FN-661, 1997.
- [6] Plum, M.A., Fitzgerald, D.H., Langenbrunner, J., Macek, R.J., Merrill, F.E., Neri, F, Thiessen, H.A., Walstrom, P.L., Griffin, J.E., Ng, K.Y., Qian, Z.B., Wildman, D., and Prichard, B.A. Jr., *Phys. Rev. ST Accel. Beams*, **2**, 064201 (1999).
- [7] Koba, K., Machida, S., and Mori, Y., KEK Note, 1997 (unpublished); Koba, K., these proceedings; Koba, K., *et al*, *Phys. Sci. Instr.*, **70**, 2988 (1999).

